

BEHAVIOUR OF VAPOUR BUBBLES GROWING AT A WALL WITH FORCED FLOW

M. G. COOPER, K. MORI† and C. R. STONE‡

Department of Engineering Science, Oxford University, Oxford OX1 3PJ, U.K.

(Received 8 July 1982 and in final form 7 December 1982)

Abstract—Experiments are reported in which individual bubbles are grown at a wall into initially isothermal supersaturated liquid moving relative to the wall, with independent control of the velocity and gravity fields. Cine observations of the bubble motion could be simply explained by non-dimensional groups involving bubble growth, fluid velocity and gravity. There was no indication of surface tension affecting overall bubble motion by causing bubbles to ‘stick’ at the wall. Thermometers on the wall surface indicated the extent of the region of dry wall below the bubble, and that was found to be smaller than suggested by other workers. The observations of previous workers may have been affected by a ‘mirage’, caused by variation of refractive index in the thermal boundary layer at the wall.

NOMENCLATURE

<p>A total surface area [m^2] A' effective base contact area [m^2] b growth parameter, $Ja \alpha^{1/2}$ [$\text{m s}^{-1/2}$] c specific heat capacity of liquid [$\text{J kg}^{-1} \text{K}^{-1}$] C_B, C_F, C_S coefficients due to buoyancy, drag and surface tension F_B, F_F, F_S forces due to buoyancy, drag and surface tension [N] g, g_e gravitational field, earth’s gravitational field h_{fg} latent heat of vaporisation [J kg^{-1}] H bubble height [m] Ja Jakob number, $(\rho/\rho_g)(c\Delta T/h_{fg})$ L length of perimeter at the triple interface [m] p pressure [N m^{-2}] r_b bubble base radius [m] R bubble radius [m] Re_x Reynolds’ number based on x, $\rho v x/\mu$ t time [s] t^* time, non-dimensionalised with (b, v) t^+ time, non-dimensionalised with (b, g) t_b base departure time [s] t_1 total departure time, ‘leaving time’ [s] t_p plate travelling time [s] T_b, T_w temperature of the bulk liquid, temperature of the wall [$^{\circ}\text{C}$] T_{sat} saturation temperature [$^{\circ}\text{C}$] ΔT supersaturation, $T_b - T_{\text{sat}}$ [K] v velocity of liquid or plate [m s^{-1}] V volume of bubble [m^3] x distance from the leading edge to the nucleation site [m] y distance normal to the boiling surface [m] Z bubble coordinate [m] Z^* Z, non-dimensionalised with (b, v)</p>	<p>Z^+ Z, non-dimensionalised with (b, g) Z_b base coordinate [m] Z_m mean position of bubble, $0.5(Z_h + Z_l)$ or $0.5(Z_u + Z_d)$ [m] Z_h, Z_l higher and lower bubble coordinates with gravity [m] Z_u, Z_d upstream and downstream bubble coordinates with flow [m]</p> <p>Greek symbols α liquid thermal diffusivity [$\text{m}^2 \text{s}^{-1}$] β liquid/solid contact angle [rad] δ boundary layer thickness [m] δ_D boundary layer displacement thickness [m] δ_0 initial microlayer thickness [m] ν kinematic liquid viscosity [$\text{m}^2 \text{s}^{-1}$] σ surface tension [N m^{-1}]</p>
--	--

1. INTRODUCTION

BOILING has long been of great importance, but owing to its complexity it is still not fully understood. One way to approach the problem is through an understanding of the behaviour of single bubbles, but even this involves several complicated phenomena. A typical bubble goes through the stages of nucleation, growth, interaction, departure, further interaction and then joins a two phase flow. All of these phenomena have been widely studied, and each may have a significant effect on boiling, at least in some cases.

Our work is primarily concerned with a part of bubble behaviour, namely growth and departure of individual bubbles at a wall, with control over the presence or absence of gravity and initial fields of temperature and velocity in the liquid. Our recent investigations [1, 2] improved the understanding of such bubbles when growing into initially stagnant liquid, with and without gravity and with known initial temperature field. It is recognised that in most practical applications of boiling the liquid is not initially stagnant, but in motion parallel to the wall. The present

† Present address: Matsui Co., Tamano, Japan.

‡ Present address: Brunel University, Uxbridge, U.K.

experiments, again with control over gravity and with initially isothermal liquid, were designed to introduce a known velocity field. Two separate experimental techniques were used to produce relative velocity: the first series of experiments used a stationary wall with a fully-developed flow of liquid past it; the second series used initially stagnant liquid, but with a wall moving. In each case, the apparatus was designed to produce a steady relative velocity after a sudden start. Observations included high-speed cine photography and simultaneous measurement of temperature (from which heat flows may be deduced) at the surface of the wall. We do not consider here phenomena of nucleation or of interaction among bubbles. Both of these have been widely studied and described in many individual papers, and nucleation has been summarised by Cole [3].

Many other workers have carried out experimental studies of developed boiling with such fluid motion, and they made various attempts at analysis based on the behaviour of the bubbles. Their experiments have been in earth gravity (usually parallel to or normal to the wall) and with interference and coalescence among many bubbles. Their analyses of the observations were therefore complicated by simultaneous interaction of many phenomena. Those analyses have typically been based on assessing forces on the individual bubbles, due to buoyancy, surface tension, 'inertia of the bubble', drag on the bubble, etc. They usually attempted to apply these analyses to the observed developed boiling. Some of the forces or influences acting on single bubbles (notably surface tension, gravity, liquid inertia due to bubble growth) are now much better understood as a result of our recent studies mentioned above. Such analyses are re-examined later in this paper.

A further complication which affects many observations but not the present work, is the formation of a mirage at a heated surface (Fig. 1). The change of refractive index inside the thermal boundary layer distorts the light paths, so that the bubble base is

obscured and a reflection of part of the bubble is seen instead [2]. The base may then appear to have area and perimeter greatly in excess of the true values. Also, the instant of bubble departure from the wall is then not observable. This is discussed below, in Section 3.3. In the present work, these problems do not arise, because the system is initially isothermal throughout. Temperature gradients will occur around the bubble, in a thermal boundary layer of order $(\alpha t)^{1/2}$, typically 10^{-4} m. Such gradients very close to the bubble may cause highly localised distortion of light paths, and perhaps exaggerate the apparent size of the bubble, if viewed with nearly-parallel backlighting. They will not cause a mirage, as shown in Fig. 1, because that depended on the light having to traverse the extended region of high temperature gradient just above the wall.

The specific aim of the present work was to characterise and quantify the influences of fluid motion and gravity parallel to the wall, and the interaction of these influences with the others examined in our previous studies.

2. APPARATUS AND PRELIMINARY WORK

2.1. General

The apparatus is sketched in Fig. 2. The 'drop table' could be raised by block and tackle, then held, and subsequently released to fall freely, or opposed by a constant force from below. It carried the test vessel and a prism and lenses, through which a stationary cine camera could take movies. The test vessel had an outer jacket with plane glass sides containing heavy liquid paraffin, heated by a controlled kettle heater element.

The inner test vessel was an inverted bell jar containing the test fluid, *n*-hexane. The internal arrangements were in some respects different for each type of experiment. In each case bubbles were produced at a glass plate on which rapidly varying surface temperatures were observed by resistance thermometers. These thermometers were in the form of thin

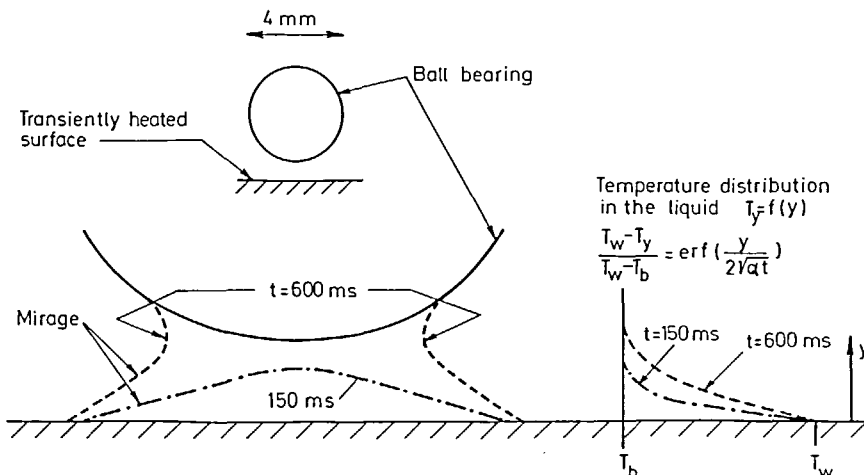


FIG. 1. Mirage formed from a ball bearing over a plate subjected to a step change in surface temperature.

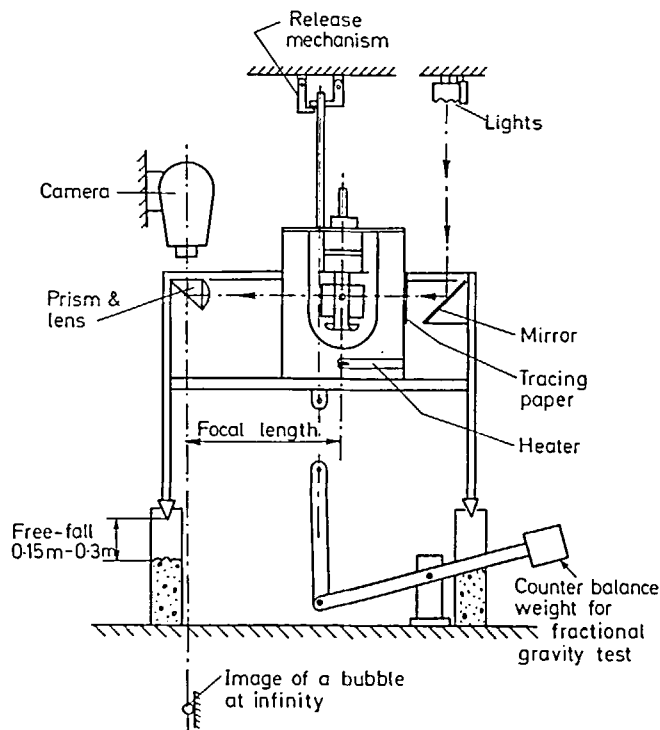


FIG. 2. General arrangement of the drop table.

films deposited onto the surface, as first used by Cooper and Lloyd [4]. Steady temperatures in the inner and outer vessels were measured by mercury in glass thermometers, that in the inner vessel being accurately calibrated.

Control and measurement of pressure were also important. A vacuum vessel was partially evacuated by a backing pump and then connected through a quick-acting valve and a reflux condenser to the test vessel. Steady pressures in the vessels before a test were observed on mercury manometers. The varying pressure in the test vessel during a test was observed by a pressure transducer.

Two different recording systems were used, as described below, and the system in use was calibrated at least once a day. In effect, this compared output from the instrumentation with the mercury thermometer or the mercury manometer.

In order to initiate the test bubble at the required time and place, one thermometer circuit was used, not as a thermometer, but as a bubble trigger. A short current pulse through that thermometer produced localised heating, sufficient to nucleate a bubble, but not greatly perturb its subsequent behaviour. Presumably this type of nucleation does form a dry spot on the wall, with a triple interface between liquid, solid and vapour, as discussed below.

In each apparatus, some tests were done with no initial relative motion between liquid and wall, and some in earth gravity by simply not releasing the table. Fractional gravity tests were obtained using the drop

table and the linkage with counterweight below it (Fig. 2) to provide a force opposing the fall. The absolute acceleration of the table was then found in separate tests in which a steel ball was projected into slow motion relative to the table at the instant of release. That relative motion was recorded on high-speed cine film, and the absolute acceleration of the table was deduced. Further details of this technique are given elsewhere [5]. The same method was used for checking its acceleration in nominally free fall. Air resistance then caused an opposing force of about 0.4% of the weight of the table, causing effective gravity 0.4% of earth gravity. During our maximum bubble life time of about 200 ms, that acceleration corresponds to a distance of less than 1 mm, which is reassuringly small compared with the size of our bubbles at that time.

Movies were taken, generally at 500 frames/s with field of view 20×25 mm. They were later projected 20 times full size to be measured to 1 mm, corresponding to 0.05 mm on the bubble.

2.2. The moving piston apparatus

The internal arrangements and mechanism are shown in Fig. 3. During a test, the piston in the upper cylinder could be raised by a rack and pinion, driven by a motor fed by a servo amplifier with velocity feedback. Test fluid from the base of the inverted bell jar was thus drawn into the smooth bell-mouth, up the glass tube (30 mm bore), and past the test plate. The test plate had sharply bevelled leading and trailing edges, and was offset in the tube, to give more room for bubble

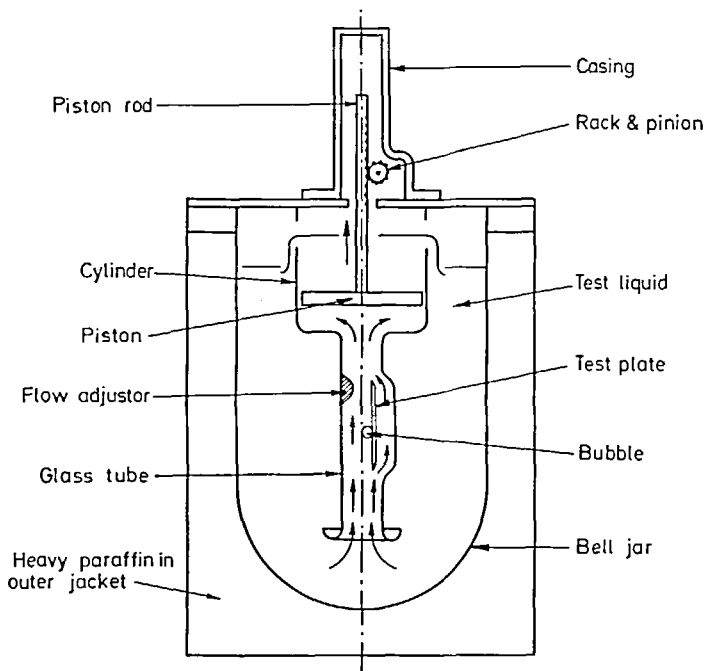


FIG. 3. Details of the moving piston apparatus.

growth. In order to ensure that fluid flowed at zero angle of incidence onto the working side of the test plate, two adjustments were made: (a) the passage at the reverse side of the plate was enlarged; (b) the flow out of the working side was slightly restricted. That restriction was adjusted by trial and error in preliminary experiments to produce the required zero angle of incidence.

In further preliminary tests with water, hydrogen bubbles were formed at a horizontal wire to mark fluid entering the tube. Photographs showed the development of the boundary layer, which corresponded closely to expectations for laminar flow [6]. In particular, the stroke of the piston before bubble nucleation was sufficient for the boundary layer to be fully developed and steady at the point of nucleation, 56 mm from the leading edge.

As a result of these restrictions etc., and also leakage past the piston (attempts at close sealing had to be abandoned because they caused unwanted nucleation), the relation between the piston velocity and velocity of the flow past the working surface was not simple. It was obtained by the hydrogen bubble technique, using water at a temperature which gave the same kinematic viscosity as hexane at the normal operating temperature.

The recording equipment was based on an ultraviolet recorder using galvanometers of frequency 8 kHz with associated bridge circuits and matching amplifiers for the thin film thermometers, and a 1.6 kHz galvanometer with amplifier for the pressure transducer. Timing circuits formed a sequence controller to operate the camera, servo motor, recorder, table release and bubble nucleation. Selected u.v. records were

digitised and replotted by computer. Further details are given in ref. [6].

Pumping a superheated liquid is difficult, as any local reduction in pressure may lead to stray nucleation. Also, in such a complicated apparatus there were many cracks and crevices which could trap undissolved gas and vapour, again leading to unwanted nucleation. As a consequence, this experiment was bedevilled by stray nucleation (especially when the table started to fall) and ultimately this led to the second experimental approach.

However, prior to this, many minor changes were made to the moving piston apparatus. The situation was improved by increasing the piston diameter and reducing the number of separate components. Under some circumstances it appeared best to let the liquid overflow from the top of the upper cylinder; on other occasions it was better to have just sufficient liquid to maintain cover over the top of the piston.

2.3. The moving plate apparatus

The idea of a plate moving through stagnant liquid had been considered originally, but rejected because some existing theories of bubble behaviour implied that the bubble would quickly move out of the field of view. However, results from the moving piston experiment showed that the bubble movement was influenced more by the bulk liquid than by the wall, so that a moving plate experiment would be feasible.

Here, the glass plate carrying the resistance thermometers was made as thin as practicable (0.8 mm), and suspended by a knife edge from the rack which had formerly been connected to the piston. Additional guidance was provided to stop the rack and plate from

rotating. The gearing on the servo motor was changed, and plate speeds up to 0.4 m s^{-1} could be obtained. The soldered connections to the resistance thermometers were at the top of the plate, always above the free surface of the liquid.

Problems with unwanted nucleation were greatly reduced, but timing was more crucial, to ensure that the plate was moving at the required speed, and the nucleation site was in the field of view immediately after the start of the fall. For these experiments the electronic equipment was designed around a 380Z microprocessor which performed two functions: timing and control of the experiment, and data acquisition. Once the pressure in the test vessel was lowered, control of the experiment was by the microprocessor. Typically that would carry out the following preliminary operations in 1 s, during which the analogue channels would be swept every 100 ms:

- (1) Switch the resistance thermometers into the measuring bridges.
- (2) Start the drop table release mechanism.
- (3) Switch on the cine lights, switch off the heater in the outer vessel.
- (4) Start the moving plate.
- (5) Start the camera.

Once the table was falling, a signal would be sent to the microprocessor, the fast data acquisition would start, and a nucleation pulse would be generated to trigger the bubble. At the end of the experiment everything would be switched off.

The rate of fast data acquisition depended on the number of channels being used. Sixteen were available, but typically six were used: for the pressure transducer, the four resistance thermometers and for time, in which case they were read about once every 0.5 ms. The analogue signals were digitised in the range 0–1023, time was recorded in units of 4×10^{-6} s, and the data were stored temporarily in RAM. At the end of each run the data could be viewed, and stored on a floppy disk. The experimental operating conditions were also stored, including the atmospheric pressure and bulk temperature. The data were then transferred to the main frame computer (DEC VAX 11/780), for processing and plotting, and finally archived on magnetic tape.

3. GENERAL RESULTS

Results are in the form of high-speed movies, normally at 500 frames/s, and high-speed records of the temperature at the surface of the plate, and of pressures in the vapour above the liquid.

3.1. Shape of bubbles

The shape of a bubble is not simple and is not fully defined by the photographs, nor would it be fully defined by photographs in two directions. No attempt has yet been made to determine the full shape; instead some key dimensions have been measured, such as Z_u

and Z_d , the positions of the upstream and downstream extremities, measured from the point of nucleation. Figure 4(b) shows how these dimensions are defined and how they vary with time in a typical case.

We again observed the phenomenon, well established by now, that a bubble which is growing reasonably fast at a wall does not sweep the wall dry below it. Instead, it leaves a thin layer of liquid (the microlayer) which it traps on the wall below. The initial thickness of the microlayer is typically a few μm , so it cannot be seen in our cine photographs. As in previous work, we infer its thickness from our high-speed measurements of temperature at the surface of the plate.

3.2. Bubble growth

It has been shown [1] that there is a simple way to describe, with acceptable accuracy, the growth of diffusion-controlled bubbles in initially stagnant isothermal liquid, despite the changes of shape due to surface tension or gravity. The description of growth is based on the ratio of volumetric growth rate, dV/dt , to full surface area A . That ratio is found to be dependent on time, but not on shape:

$$\frac{(dV/dt)}{A} \approx b/t^{1/2}$$

where

$$b = Ja \alpha^{1/2}$$

and

$$Ja = \rho_l c_{pl} \Delta T / (\rho_g h_{fg}).$$

This equation fully describes diffusion-controlled bubble growth, without the need to know individually the thermal properties, conductivity, latent heat, etc. or superheat. The only information needed from the energy equation is $b = Ja \alpha^{1/2}$. This has been used successfully [1] to set up a dimensionless time for the transition from hemispherical shape to spherical shape, due to the change in relative importance between inertia stresses from bubble growth and surface tension stresses.

In the experiments reported here, this relation cannot be checked because volume and area are not measurable. However it does again seem to give a reasonable description of bubble growth, despite even more complex changes of shape. We use that fact, not as an accurate description of bubble growth, but as an indication that the information needed from the energy equation is again summed up in the parameter $b = Ja \alpha^{1/2}$.

3.3. Bubble departure

This work makes it clear that, in the very common case of gravity and/or fluid flow parallel to a wall, the definition of time of departure presents a problem. The bubble normally grows at first almost symmetrically about the point of initiation, then distorts and eventually moves along the wall (upwards or downstream). It appears to roll or slide along the wall,

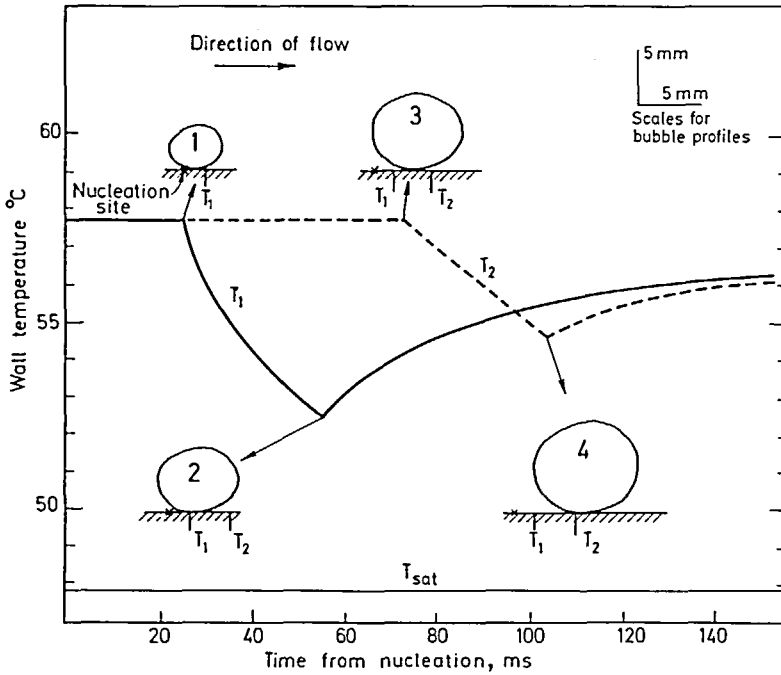


FIG. 4. Vapour bubbles grown on a stationary plate with forced flow in zero gravity; $v = 0.103 \text{ m s}^{-1}$, $Ja = 25.0$: (a) Wall temperature and saturation temperature variations, with bubble profiles; (b) Variation of the upstream and downstream coordinates.

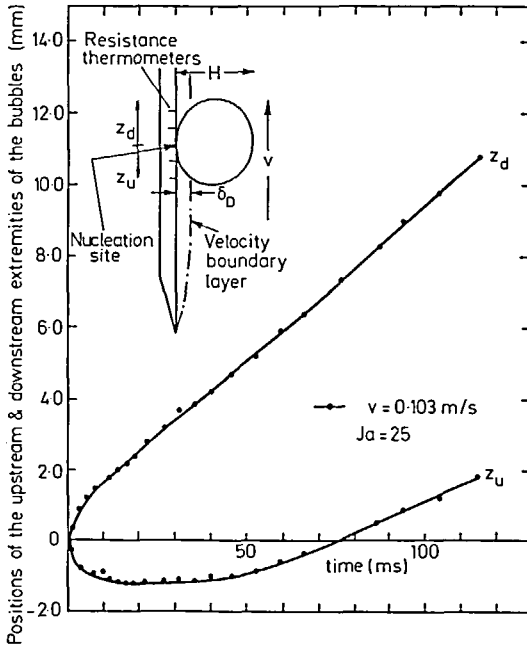


FIG. 4(b).

forming a 'wedge' of liquid, thicker than the microlayer, between it and the wall. The details of the wedge would not be seen if there were a mirage (Fig. 1).

It is not clear what 'time of departure' means in such cases. In a sense, the bubble is in true contact with the

wall only during the period (normally very short) when vapour is at the wall. It may appear to be at the wall when in fact a thin layer of liquid is there: initially the microlayer or part of it; subsequently the wedge. An arbitrary definition could be set up, e.g. that 'departure' means that the wedge is nowhere less than a certain thickness. In the simple mirage of Fig. 1, departure would appear to occur when the bubble is just above the top of the mirage—about the top of the thermal boundary layer. Many previous studies must have recorded this as departure.

In this study, we record two times t_b and t_l , which can be clearly identified from the movies. The suffixes refer to base and leaving. Time t_b is when the base of the bubble appears to have moved entirely downstream of the nucleation site; t_b could not be observed if there were a mirage. Time t_l is when the whole of the bubble has moved downstream of the nucleation site. In Fig. 4(a), four tracings are given, showing that t_b occurs at about the time of tracing 1, and t_l occurs at about the time of tracing 3. The latter can be more accurately observed.

Many previous analyses of heat transfer in boiling have required a departure time, which was used in various ways, depending on the heat flow mechanism assumed to predominate. For such heat flow studies, it might be useful if our work could establish a time beyond which the bubble had little influence on heat flow from the wall, whether in its region of nucleation or elsewhere. That is not such a clear definition, but it is discussed below.

4. RESULTS IN ZERO GRAVITY

The two experimental methods for flow relative to the wall in zero gravity enabled a wide range of conditions to be covered. Jakob number was in the range $4.6 < Ja < 48$, and relative velocity was in the range $0.045 < v \text{ [m s}^{-1}\text{]} < 0.39$.

4.1. Moving piston results

Figures 4(a) and (b) refer to a typical bubble in zero gravity. As discussed above, the tracings in Fig. 4(a) show $t_b, t_1 = 25, 75$ ms respectively, the latter confirmed by the axial intercept in Fig. 4(b).

The graph in Fig. 4(a) shows the temperatures observed by the surface thermometers at the points indicated. They show no variation until a short time after the bubble base covers the thermometer, then fall while the base is covering it, then rise again after the base has moved away downstream. The output from the pressure transducer is plotted on the same graph, as saturation temperature. It shows little variation.

4.2. Discussion of the moving piston results

It is readily seen from Figs. 4(a) and 4(b) that the bubble grows at first somewhat like the parabolic

relation $R = 3 Ja (\alpha t)^{1/2}$, obtained with hemispherical diffusion-controlled bubbles in stagnant isothermal liquid. Also, the advance of the downstream extremity eventually approaches a steady velocity, close to the main stream velocity v . These two observations suggest that the results might fall conveniently on a common plot involving dimensionless groups, determined from the following reasoning.

Here, the dominant phenomena appear to be initially the normal bubble growth, and subsequently the motion of the main stream, characterised by b and v respectively. If we now form non-dimensional time t^* and non-dimensional distance Z^* using b and v , we can only have

$$t^* = \frac{t}{(b/v)^2} \quad Z^* = \frac{Z}{(b^2/v)}$$

In terms of these, $Z = 3b t^{1/2}$ becomes $Z^* = 3 t^{*1/2}$, and drift at velocity v becomes $Z^* = t^*$. As that suggests, the observed values of Z_u and Z_d for a wide range of bubbles do indeed fall closely together when plotted as Z_u^* and Z_d^* against t^* (Fig. 5). There is appreciable scatter here and on similar graphs, so error bands are shown which contain 60% of the readings and

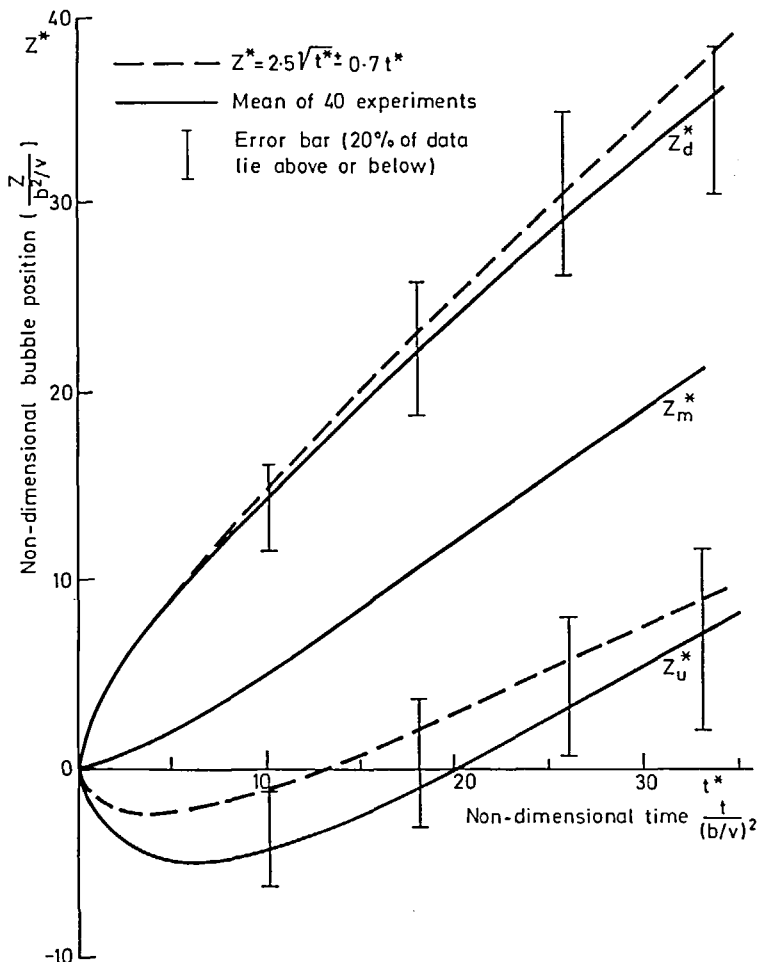


FIG. 5. Non-dimensional motion of vapour bubbles with forced flow over a stationary plate in zero gravity.

therefore would correspond broadly to a range of one standard deviation on each side of the mean if the scatter followed a Gaussian distribution.

Thus these parameters Z_u and Z_d , which are major indicators of the overall movement of the bubble, appear to be strongly influenced by bubble growth (b) and main stream velocity (v), but not strongly influenced by other quantities such as viscosity and surface tension. This contradicts the common assertion that surface tension is a significant factor in determining the motion of such bubbles.

It is not suggested that viscosity and surface tension have no influence. Indeed viscosity will surely affect fluid motion very close to the wall, e.g. under the bubble, and in the velocity boundary layer. It gives rise to a further dimensionless parameter, such as b^2/v , which is Ja^2/Pr , which varies widely as Ja is varied from 4.6 to 48. If it has an effect, then it would influence the common plot (Fig. 5). No influence of that group has emerged, though there might be an effect which is obscured by systematic variation of Ja across Fig. 5. Surface tension will influence the degree of rounding off and thus alter the numerical constant 3 above, since that applies for a hemispherical bubble, whereas 2 applies for a spherical bubble. The effects of surface tension can be emphasised by experiments with slowly growing bubbles in slowly moving liquid. However, in this apparatus the bubble would then be small

compared with the velocity boundary layer, and that too will have an effect.

Attempts were made to determine the effect of the velocity boundary layer. For this purpose, a measure of the translation of the bubble as a whole was defined. That is the mean of the upstream and downstream coordinates, $Z_m^* = (Z_u^* + Z_d^*)/2$. It can be seen from Fig. 5 that dZ_m^*/dt^* eventually reaches about 0.7. Less clearly it can be seen that dZ_m/dt is initially zero. It may be expected that the transition from 0 to 0.7 v will occur as the height of the bubble grows from much less than to much greater than the thickness of the velocity boundary layer. The boundary layer can be conveniently represented by its displacement thickness δ_D , which, for a fully developed laminar boundary layer at a point x from the leading edge is

$$\delta_D = 1.73x/Re_x^{1/2}$$

where

$$Re_x = vx/\nu.$$

The results from many bubbles are plotted in Fig. 6, in the form of $Z_m/(vt)$ against H/δ_D . The results are scattered, particularly at low values of H/δ_D , but nevertheless it can be seen that once the bubble height is about 5 times the displacement thickness, the motion is dominated by the main stream, and Z_m increases at about 0.7 v .

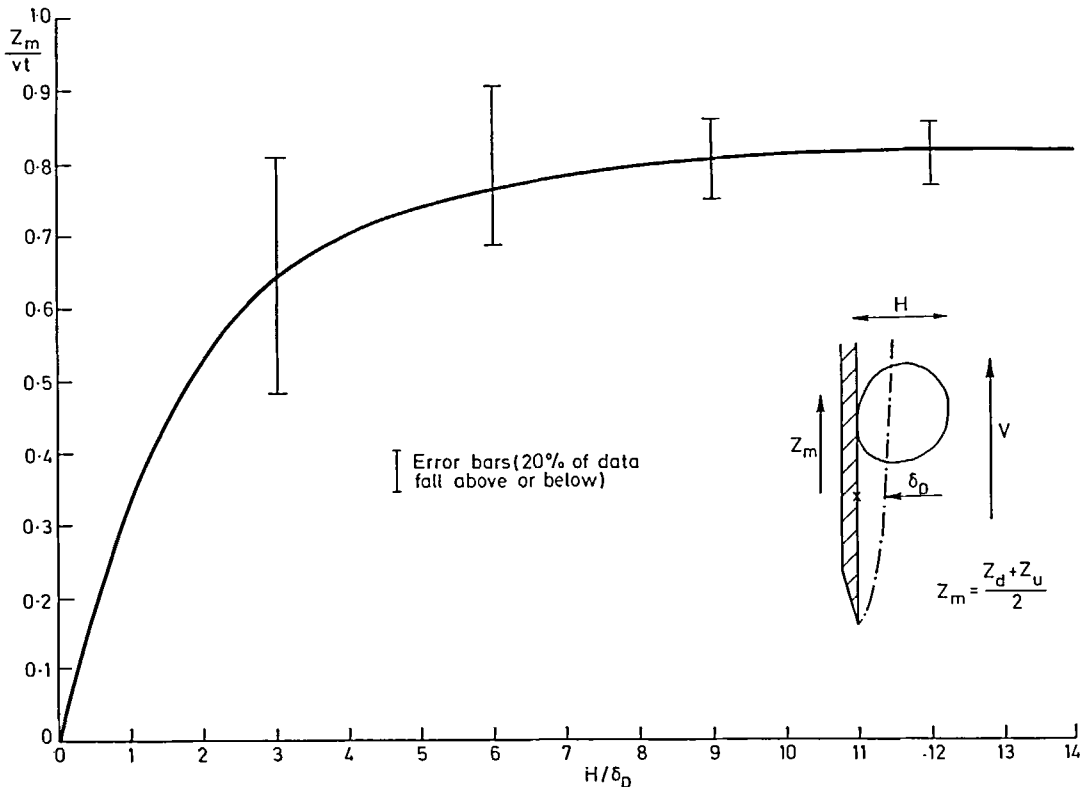


FIG. 6. Bubble motion/(fluid motion) as a function of bubble height and boundary layer thickness for forced flow over a stationary plate in zero gravity.

4.3. Moving plate results

The results from the moving plate experiment corroborate the results from the moving piston experiment. However, higher superheat could be used without causing unwanted nucleation, there were some minor differences, and some more details could be determined, particularly concerning the dry area under the bubble.

Existing theories often assume that, under the bubble, there is a large dry area (its apparent large size may often have arisen from a mirage), and that surface tension at its perimeter has an important influence on bubble motion. No dried-out region had been detected in the tests with a moving piston, although our method of nucleation must form some dry spot. In the hope of observing dry-out, higher ΔT and hence Ja was used, and the distance between the resistance thermometers was halved to 0.75 mm. Figure 7(a) shows the outputs from three of the resistance thermometers, with the saturation temperature again derived from the pressure transducer. For the innermost thermometer, the surface temperature has fallen to saturation temperature at 13 ms, indicating that the microlayer has been completely evaporated by heat diffusing from the wall. After that dry-out, the wall temperature rises as heat continues to flow from inside the wall faster than it can be removed by the vapour. At about 34 ms there is a rapid fall in temperature as the bubble base moves past that thermometer, so it is again exposed to the liquid. (This fall re-confirms the occurrence of dry-out.) Finally the temperature recovers towards the bulk value. At the second thermometer, 1.5 mm from the point of nucleation, dry-out and base departure both occur at about 41 ms. The third thermometer (at 2.25 mm) does not dry out; while the bubble base is over that thermometer, heat from the solid flows through the microlayer to the evaporating interface, but there is insufficient time to evaporate the microlayer com-

pletely. Once the bubble base has moved past that thermometer (about 48 ms) the temperature recovers. Thus a dry spot does occur, but it does not reach the third thermometer, so its size is small compared with the bubble size, and it will be shown later that it does not appear to cause the bubble to 'stick' as some theories suggest.

Estimates of the initial microlayer thickness, using those temperature readings in a 1-dim. numerical model of heat conduction, give thicknesses consistent with the results from bubbles in stagnant liquid. This is not surprising, as the microlayer is thin compared with the velocity boundary layer, and this part of the microlayer is formed at the stage of rapid radial growth (i.e. $dR/dt \gg v$).

4.4. Discussion of the moving plate results

Again the bubble grows at first almost symmetrically about the point of nucleation. Later it moves slowly in the same direction as the plate [Figure 7(b)].

The same dimensional arguments apply as before, but the measurements in this case are based on a datum fixed in the bulk liquid. Figure 8 shows the variation of the non-dimensional mean displacement, Z_m^* ; scatter is large, because it is obtained from the difference of two nearly equal numbers, Z_u and Z_d . Nevertheless, it can be seen that the bubble moves at about 0.1 times the plate velocity; there did not appear to be any segregation based on either growth rate or plate velocity; there was no appearance of the bubble sticking to the wall and moving with it.

The effect of the velocity boundary layer was again considered. In these experiments the velocity boundary layer develops continuously with time, as momentum diffuses from the wall, governed by the kinematic viscosity. The velocity field is $v \operatorname{erf}[y/(2\nu^{1/2}t^{1/2})]$ and the displacement thickness $\delta_D = 2(\nu t_p/\pi)^{1/2}$, where t_p is the duration of plate travel. In general, the plate travel

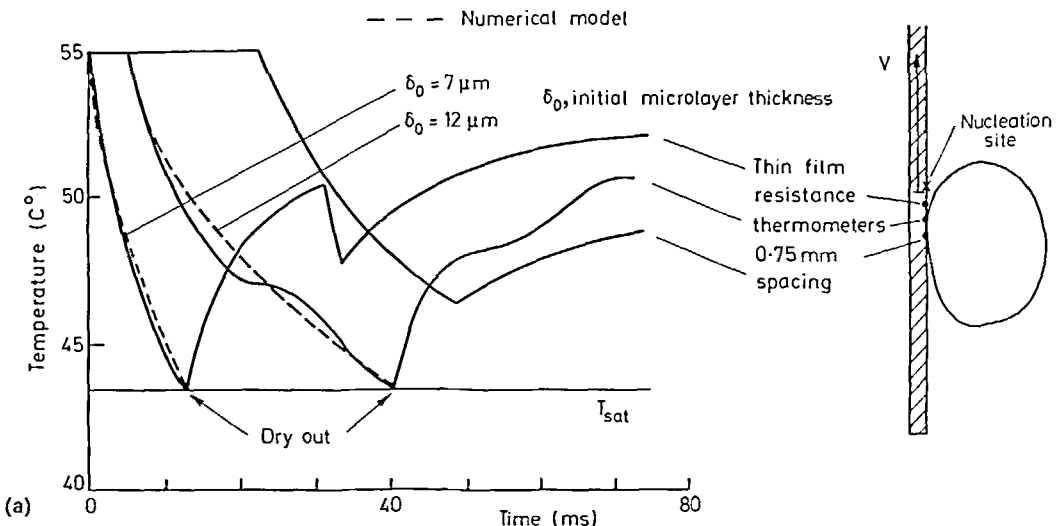


FIG. 7 (continued overleaf).

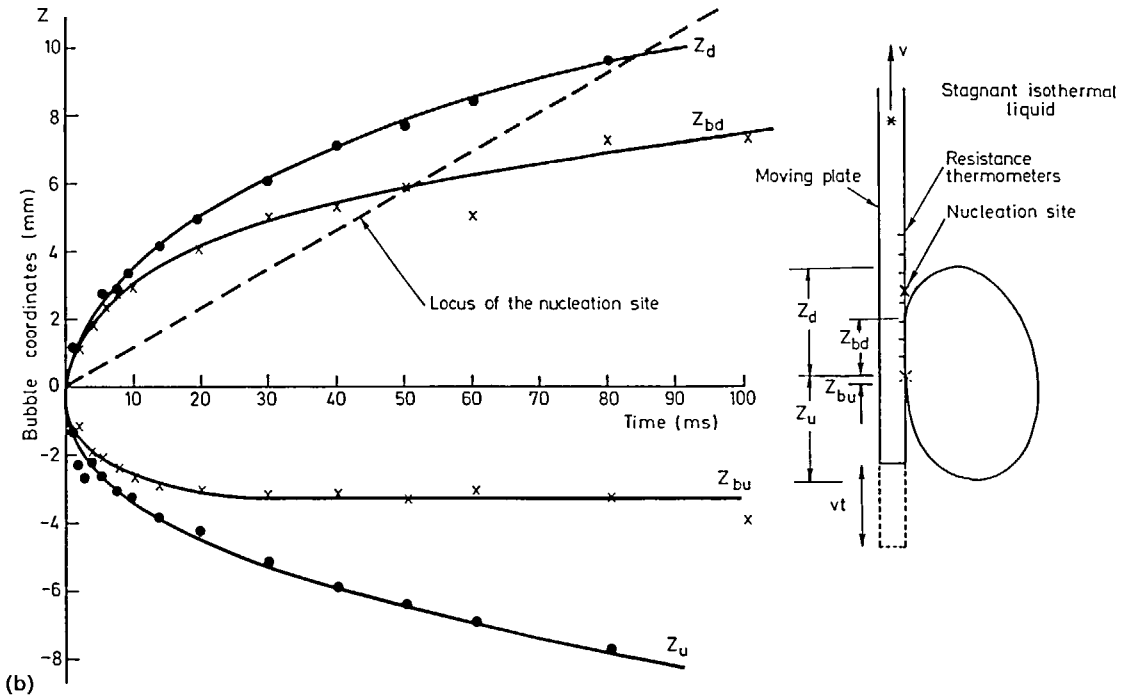


FIG. 7. Vapour bubble grown in stagnant liquid on a moving plate in zero gravity; $v = 0.115 \text{ m s}^{-1}$, $Ja = 33.0$: (a) Wall temperature and saturation temperature variation, comparison with numerical microlayer evaporation model. (b) Variation of bubble dimensions.

time was large compared with the duration of bubble growth, so that changes in δ_D were small during bubble growth. As shown in Fig. 9, once H exceeds about $5 \delta_D$, the bubble moves at less than 0.2 times the plate velocity. Subsequent behaviour may differ, between Fig. 9 and Fig. 6, but it was not pursued, because the

moving plate tests are not a practical case; they had achieved their intended objective of confirming, over a wider range of conditions, that the bubble motion is dominated by the bulk liquid. The bubble either slips readily over the wall, or allows the wall to slip readily below it.

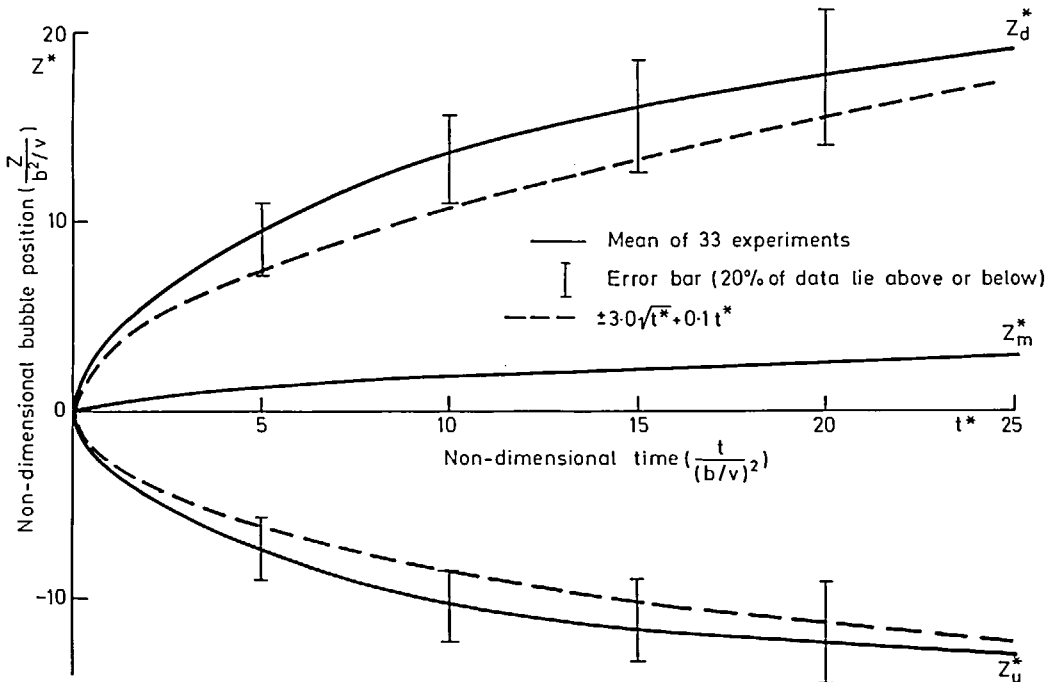


FIG. 8. Non-dimensional motion of vapour bubbles on a moving plate in stagnant liquid and zero gravity.

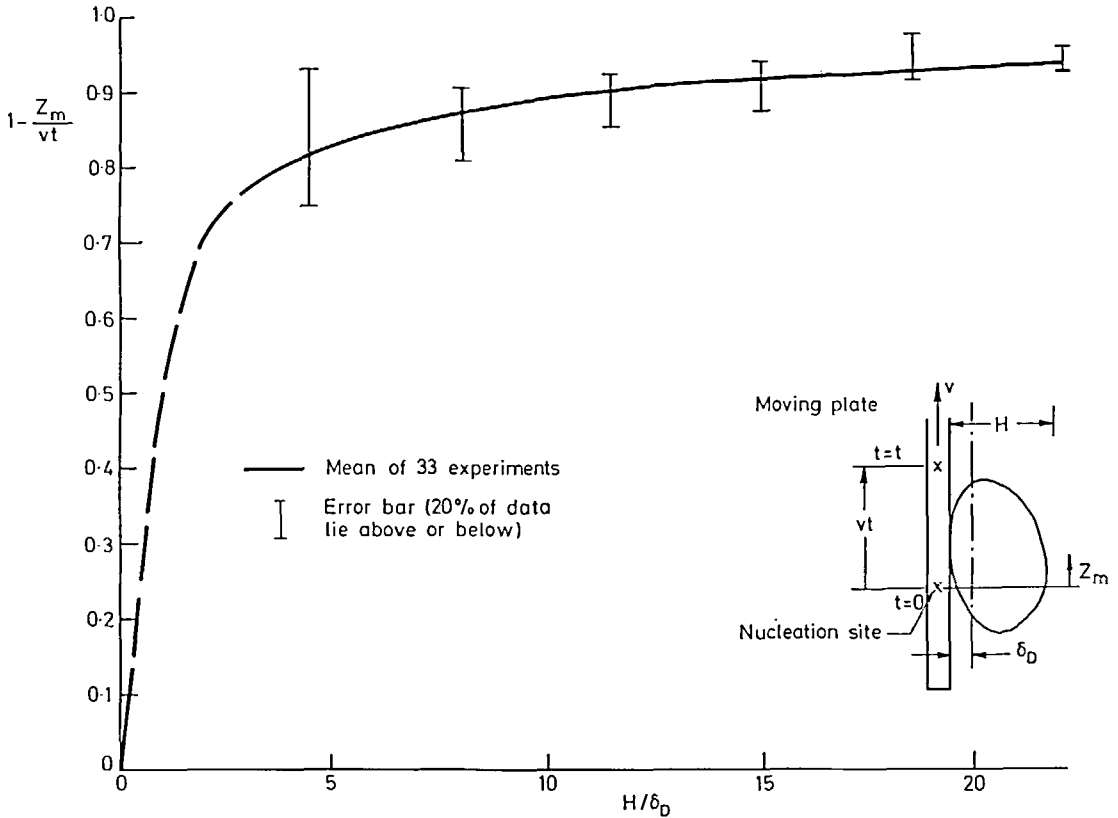


FIG. 9. Bubble motion/(fluid motion) as a function of bubble height and boundary layer thickness for stagnant liquid with a moving plate in zero gravity.

5. RESULTS WITH EARTH GRAVITY OR FRACTIONAL GRAVITY

Tests were also carried out with a combination of gravity (full or fractional), and with the piston or plate stationary or moving. Parameters were varied to see if any 'sticking' of the bubble could be observed with the buoyancy force reduced by fractional gravity.

5.1. Stationary vertical plate results

Tests were conducted with no relative motion between the plate and the bulk liquid, with wide ranges of Ja ($8 < Ja < 40$) and gravitational acceleration ($0.02 < g/g_e < 1.0$), parallel to the plate. The results followed a simple pattern. Initially the shape of the bubble did not appear to be greatly disturbed by gravity, and the bubble grew almost symmetrically about the nucleation site. Subsequently the bubble moved appreciably, and ultimately it became distorted. Tracings of the bubble profiles are shown in Fig. 10(a), together with the corresponding wall temperature and saturation temperature responses. The initial falls in wall temperature are compared with those derived from a 1-dim. numerical model of microlayer evaporation with no convection.

Again, no attempt was made to determine the full shape, instead the vertical coordinates of the higher and lower extremities of the bubble (Z_h, Z_l), and its base (Z_{bh}, Z_{bl}), were measured from the nucleation site.

Figure 10(b) defines these dimensions, and shows how they varied with time. As before, departure from the wall was ill-defined, but times t_b, t_1 can again be determined.

5.2. Discussion of the stationary vertical plate results

Dimensional arguments can be used, as above, noting that here there is no relative velocity v between the bulk liquid and wall, but gravity g is present. If b and g are the only significant influences, the non-dimensional groups for distance Z and time t can only be

$$Z^+ = \frac{Z}{(b^4/g)^{1/3}} \quad \text{and} \quad t^+ = \frac{t}{(b/g)^{2/3}}$$

distinct from those used when velocity was present and gravity absent.

In terms of these groups, parabolic growth $Z = 3b t^{1/2}$ becomes $Z^+ = 3t^{+1/2}$, and displacement with acceleration g becomes $Z^+ = 0.5t^{+2}$. Using these groups, all data could be plotted on a common graph (Fig. 11).

Ultimately the bubbles would reach a terminal velocity ($Z^+ \propto t^+$), but this was only apparent for the tests in full gravity. The terminal motion of freely rising vapour bubbles has been widely studied, but was not the objective of this work. (Batchelor mentions many works on rising gas bubbles [7].) Florschuetz *et al.* [8]

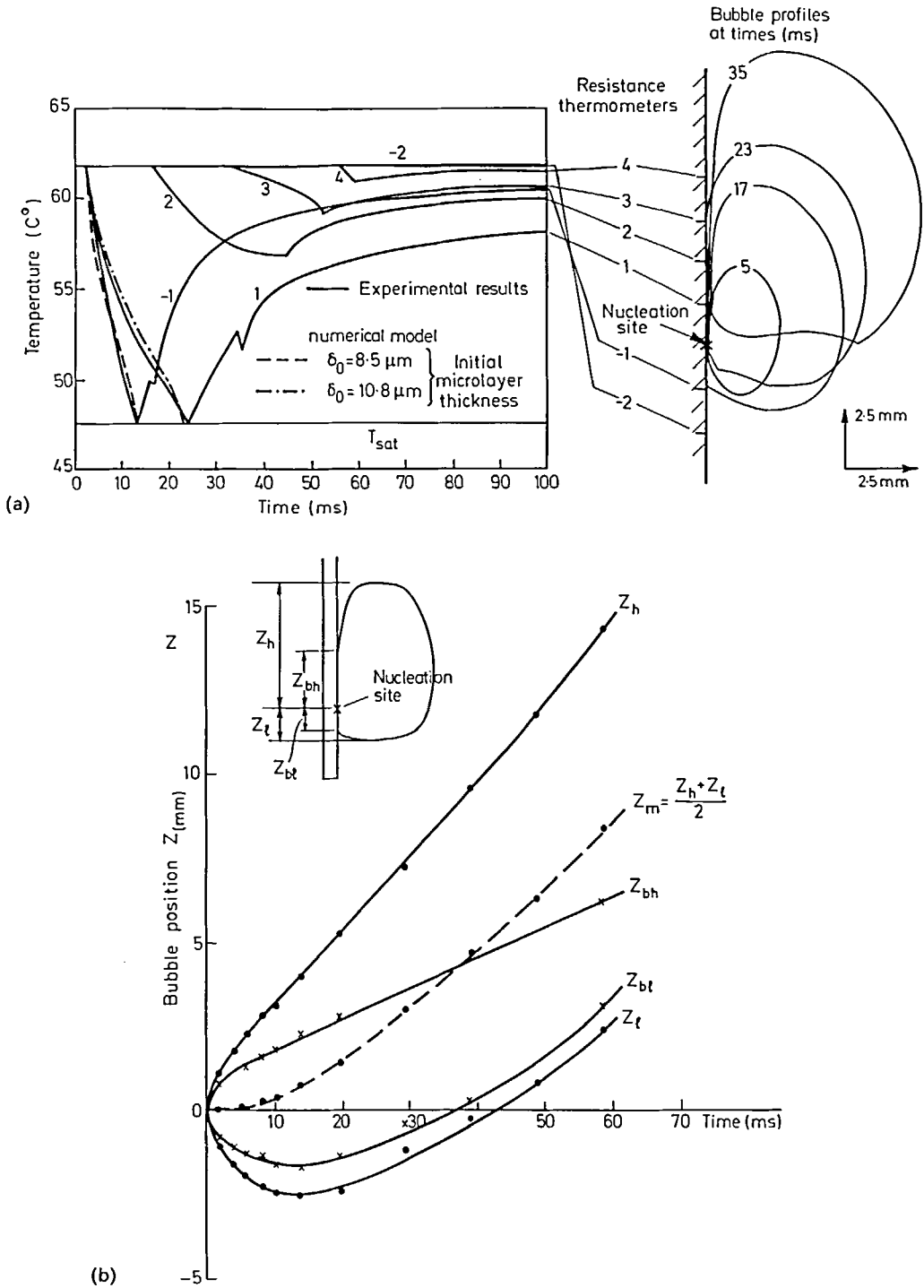


FIG. 10. Vapour bubble grown on a stationary vertical plate in stagnant liquid with earth gravity; $Ja = 36.9$: (a) Wall temperature and saturation temperature variation, comparison with the numerical model, tracings of the bubble profiles. (b) Variation of bubble dimensions.

have investigated how the growth of vapour bubbles is affected by motion through initially stagnant isothermal liquid in earth gravity.

The early, transient bubble motion was again examined closely, using the mean bubble position Z_m , defined as the mean of the upper and lower coordinates.

Motion controlled solely by gravity would imply $Z_m^{1/2} \propto \text{time}$, or a straight line on Fig. 12 passing through the origin, $Z^{1/2} = (0.5g)^{1/2} t$, or $Z^{+1/2} = (0.5)^{1/2} t^+$. A straight line is indeed found, as $Z_m^{+1/2} \approx (0.25t^+)^{1/2}$, an upward acceleration about 50% of gravity.

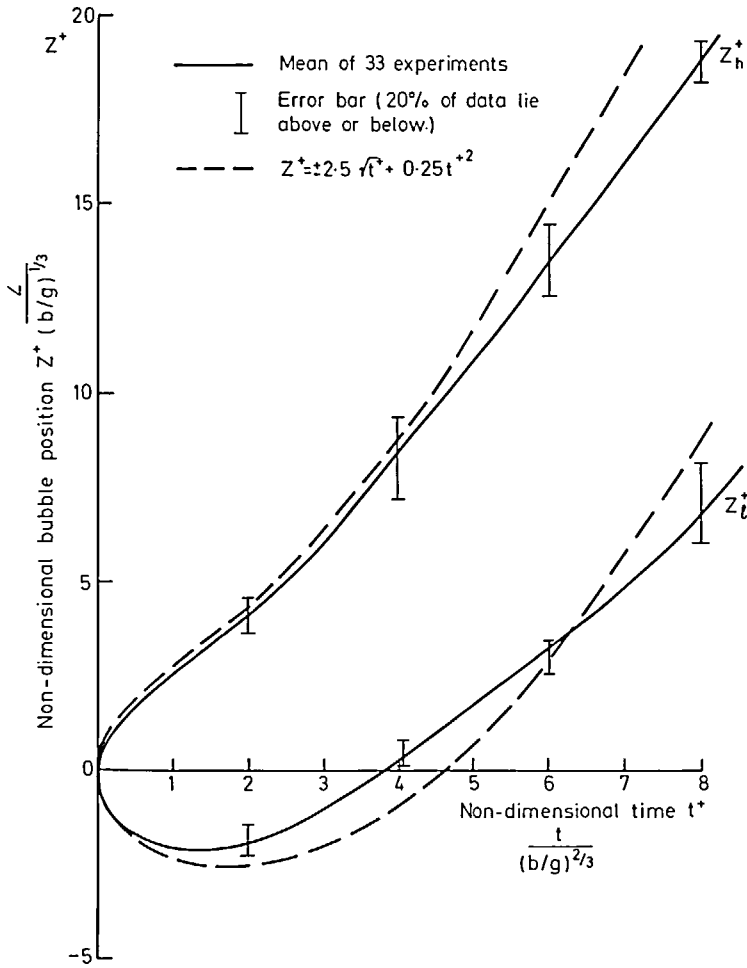


FIG. 11. Non-dimensional motion of vapour bubbles grown on a stationary vertical plate in stagnant liquid with fractional and earth gravity.

Scatter is inevitable in Fig. 12, particularly near the origin, as Z_m is the difference of two nearly equal numbers, particularly for small values of time when the numbers are also small. Further, at the initial stage any effect due to gravity will be small. After 10 ms the characteristic length ($0.5gt^2$) due to full gravity g_e is about 0.5 mm. In fractional gravity of 2% g_e , the distance would be 0.01 mm, whereas measurements of bubbles were to 0.05 mm, as described above.

It is noteworthy that the line in Fig. 12 implies acceleration about 50% of gravity. Simple arguments using buoyancy force and the virtual mass of a sphere in infinite liquid (half the mass of liquid displaced) would imply upward acceleration of twice gravity, and that has been observed by others [9]. The reduced acceleration shown in Fig. 12 suggests the wall has a drag effect, which could be caused by viscous forces in the liquid wedge between the bubble and the wall. The drag force reduces acceleration, but it is not the same as 'sticking' due to surface tension. Sticking is more likely if stresses other than those from surface tension are reduced. To encourage sticking, we grew bubbles with gravitational field reduced to 2% of earth gravity, and

with growth rate slow, but sufficient for dry-out to be observed at some thermometers. It was possible to see that a small area of the bubble base was subject to sticking, as it caused local distortion of the bubble, but even in this most extreme case there seemed no possibility of significant effect on departure time. In other cases, with stronger gravitational field, or with relative velocity, there was no indication of sticking at all.

5.3. Moving piston results with gravity

Results with both flow and gravity were obtained by operating the moving piston apparatus without releasing the drop table. The glass plate was mounted vertically and the flow was vertically upward, as is usually the case in forced flow boilers. Jakob number and velocity were in the ranges $8 < Ja < 48$, $0.075 < v$ [m s^{-1}] < 0.61 . The velocity boundary layer was always fully developed. Again, the coordinates of upstream and downstream extremities were measured.

5.4. Discussion of moving piston results with gravity

The simplest possible combination of previous results, ignoring the effect of the velocity boundary

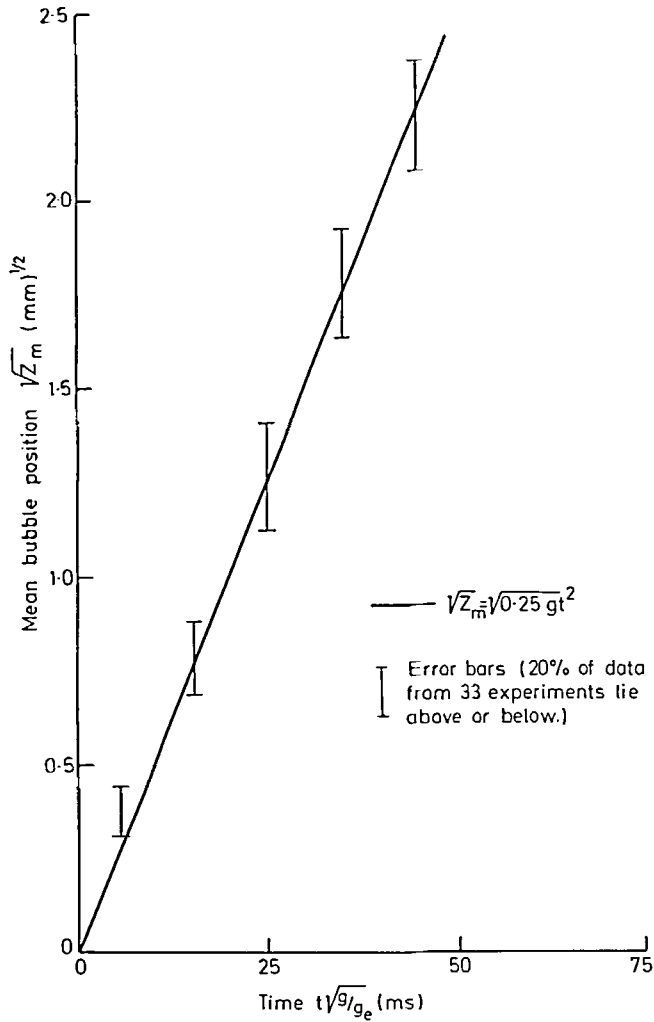


FIG. 12. Mean position of bubbles grown on a vertical plate in stagnant liquid, plotted against time. Bubbles accelerate with no indication of 'sticking'.

layer and terminal velocity, would be linear addition (superposition) leading to

$$Z_d = 2.5bt^{1/2} + 0.75vt + 0.2gt^2,$$

$$Z_u = 2.5bt^{1/2} + 0.75vt + 0.2gt^2,$$

$$Z_m = 0.75vt + 0.2gt^2,$$

and, as shown in Fig. 13(a), these appear to give a reasonable first approximation to the early observations, though fractional scatter is appreciable, particularly for Z_u which passes through zero. It is again possible to distinguish stages of the process as the various terms predominate in sequence: while $2.5bt^{1/2}$ dominates, the bubble grows at normal rate with little translation; while $0.75vt$ dominates, the bubble moves as expected in flow without gravity; when $0.2gt^2$ dominates, the bubble moves as expected under gravity without flow. The abscissa in Fig. 13(a) is chosen to distinguish these last two regimes, as they correspond respectively to low and high values of gt/v (= the length ratio gt^2/vt).

The motion is clearly more complex than this simple discussion suggests; early motion is affected by the velocity boundary layer, the stages overlap and are finally superseded by approach to a terminal velocity. Nevertheless, as indicated by Fig. 13(a), the actual values of Z_d and Z_m during our periods of observation were generally between 1 and 1/2 of these simple predictions. Closer examination of Z_m can show the effect of velocity boundary layer on the early motion. This is illustrated in Fig. 13(b), where $Z_m/(0.75vt + 0.2gt^2)$ is plotted against H/δ_D . As in Figs. 6 and 9, once the bubble height is about five times the displacement thickness, the motion is again dominated by the mainstream and gravity fields.

6. COMPARISON WITH OTHER WORK

6.1. Analyses of bubble departure

The form of these results is not in accordance with previous analyses of bubble departure based on a force balance for an individual bubble, involving terms F_B ,

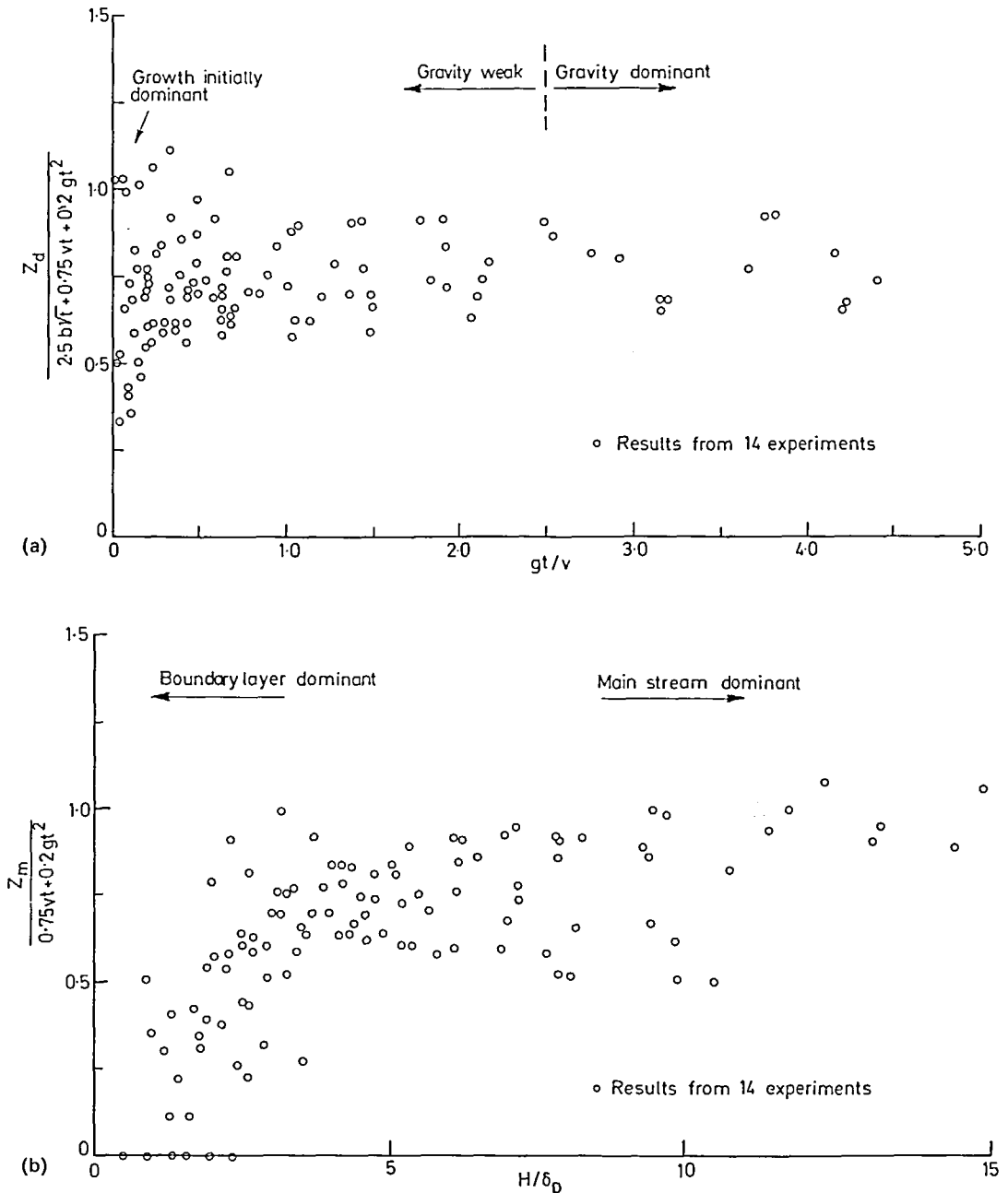


FIG. 13. Experiments with a stationary vertical plate, forced upflow and earth gravity: (a) Variation of bubble coordinate with time. (b) Motion of the bubble as a function of bubble height and boundary layer thickness.

F_S , F_F , due to buoyancy, surface tension and friction or drag. These terms are generally expressed as $F_B = C_B(\rho_f - \rho_g)gV$ where V is bubble volume; $F_S = C_S \sigma L \cos \beta$ where L is a length, of order cavity radius or bubble radius and β is some form of contact angle; F_F is variously $C_F (-dp/dz)V$ ([10], vertical wall) or $C_F(\rho v^2/2)A$ where A is an effective area ([11], horizontal wall). Coefficients C_B , C_S , C_F were generally adjusted to suit experimental results. In some cases C_F was based on drag for a sphere at the same Re , although such drag phenomena depend on fully developed flow with

wakes. Wakes can occur with bubbles, and are often observed below buoyant rising bubbles, which then become distorted unless they are very small. Wakes could not be established in the short times of our experiments, nor indeed during the short life (before departure) of many bubbles in boiling. A wake cannot start to develop until the downstream extremity of the bubble is moving slower than the main stream (slope less than 1 in Fig. 5). Some time thereafter, the region of reversed flow can presumably spread upstream from the downstream extremity, to create separation of flow

and a wake. Our experiments show little or no sign of the distortion to be expected if there were wakes, as mentioned above.

Our experiments are apparently the first to study individual bubbles under conditions which are sufficiently controlled to provide a test of the theories. Previously, the parameters of the model such as C_B , C_S , C_F were found by appeal to observations of fully developed flow boiling, where bubbles interact and other effects arise.

In one such study [10], a sketch shows a length r_b , characterising bubble size and also (of similar order) base size. Comparison with developed flow boiling showed F_B to be negligible, leaving $F_S = F_F$, where F_S was taken as $C_S \sigma r_b$ and F_F was taken as $C_F (-dp/dz) r_b^3$ with dp/dz from a standard friction formula, and further comparison with experiment showed $C_S/C_F = (0.015)^2$. Since F_F on this theory can hardly exceed $(-dp/dz)V$, there is an upper bound on C_F and hence on C_S , apparently $C_S < 0.003$. This implies that, if the observed departure was in fact due to a balance between F_B and F_F , then $L \cos \beta$ must be of order $0.003 r_b$, which suggests that the base was several orders of magnitude smaller than r_b , or that departure was not in fact governed by the assumed force balance.

Analyses which include forces related to 'equivalent mass', i.e. inertia in the liquid due to the motion of the bubble, could be compatible with our findings, but equivalent mass originates from the very simplified case of frictionless flow around a sphere in infinite liquid, with some possible extensions, such as for a sphere moving near a wall. It is also possible to derive a force related to the increase in liquid momentum needed to maintain the velocity of a bubble despite growth, again for a sphere in infinite, inviscid liquid. Such forces could be adapted here, but the matter really concerns the combined effects of acceleration and growth, which do not appear to have been studied, even for a sphere in infinite inviscid liquid. It would also be necessary to introduce additional parameters to allow for the great effects of the wall and velocity boundary layer.

By combining various aspects of these existing analyses, with many disposable parameters, a fit could surely be obtained to our data, but we are not confident of the value of such an exercise, since the set of parameters would not be unique. The problem really requires full examination of the motion coupled to the energy equation, all with moving free surfaces of unknown shape, but that is expected to remain beyond analysis or computation for some time to come. It may be useful to undertake interim analyses of fluid mechanics with simplified assumptions concerning bubble growth and bubble shape, but such problems are by no means trivial.

6.2. Analyses of heat flow

There are various theories to explain why heat flow in nucleate boiling exceeds that in single-phase flow. Some argue that there is a rapid flow of heat more-or-less directly from the wall into the bubble through a

microlayer or otherwise, before 'bubble departure'. Other theories attach more weight to enhanced transfer of heat from wall to liquid, due to pumping action of the bubble, or microconvection or otherwise, largely after 'bubble departure'. There is no precise dividing line between these theories, since heat flow is strictly from wall to liquid in virtually all cases. In the wording above, the theories are roughly divided by being before or after 'bubble departure'. As was explained earlier, the present work suggests that the physical departure of the bubble is ill defined, but it may be possible to indicate an order of magnitude for the time and the area over which appreciable amounts of heat flow fairly directly into the bubble.

6.3. Experimental work

The experiments reported here concern bubbles grown in a uniformly superheated liquid though we have conducted experiments with a known temperature field [2], without, as yet, a velocity field. Most experiments by other workers have been in the normal engineering situation with liquid flowing past a heated wall [liable to cause a mirage (Fig. 1)], and with the liquid subcooled or saturated. Nevertheless they are examined below for comparison with our results, as regards sliding velocity and the tendency for bubbles to remain at the wall. A few results exist which enable such comparison. We have found no other work to compare with our observations of bubble acceleration and the effect of the velocity boundary layer in boiling.

6.3.1. *Sliding velocity.* Gunther [12] conducted flow boiling experiments with a high degree of subcooling in water. He was mainly interested in the conditions which influenced burnout, but he reported that the bubbles slide at about 0.8 of the mainstream velocity. Akiyama and Tachibana [13] report bubbles sliding at 0.3–0.8 of the mainstream velocity. Williams and Mesler [14] investigated delay time between bubbles on a horizontal and a vertical heated copper surface in stagnant saturated water. Neither the wall temperature nor the heat flux was reported; the results are in the form of tracings from cine films. Measurements taken from the three sequences of bubbles growing on a vertical surface are consistent with our results for bubble motion along the wall.

6.3.2. *Bubble growth and tendency to depart.* Departure of bubbles from a wall is dependent on initial temperature gradients, as shown in ref. [2] for individual bubbles in initially stagnant liquid. In that work, attempts were also made to devise a simple expression for growth. One approach was to combine evaporation from the base (microlayer), with the slower evaporation or condensation at the upper curved surface, bearing in mind previous analyses [15]. Due partly to the impossibility of observing the base accurately through the mirage, no such expression could be devised, even for that simple case. However, if

we take the case when a given superheat (say 10 K) applies throughout the liquid, and compare that with the case where the superheat is 10 K at the wall and lower in the liquid, then the second case naturally causes slower growth. The growth is not only slower, but it also has some different characteristics, including an element of deceleration. For that reason, or otherwise, it has been found that [2], even in zero gravity, the bubble leaves the wall, whereas it did not leave convincingly when grown in an initially isothermal liquid. Such departure, 'unaided by gravity', has been reported by various observers in pool boiling. In flow boiling, Gunther [12] reports the contrary, as he found that bubbles slid along the wall. Kirby *et al.* [16] found a similar sliding if heat flux was high, but the bubbles did depart if the heat flux was less than about 10% of the Critical Heat Flux, and the subcooling was less than 5 K. A possible further factor here is thermocapillarity, which can cause bubbles to move up a temperature gradient. The higher surface tension on the colder part of the bubble surface draws the surface and adjoining liquid towards the cold region, so propelling the bubble towards the hot region. It would be interesting to investigate this change in behaviour (leaving the wall or not), by conducting experiments on individual bubbles in a liquid having both a temperature and a velocity field. It might be expected to affect the heat flow from the wall. An initial temperature field and the consequent altered growth, discussed above, may also have an indirect effect on the likelihood of 'sticking', by affecting the size of the dry area and the forces due to buoyancy and passing fluid. Again, this is a matter for experiment, and theoretical arguments are not clear at this stage.

In our experiments, the bubble size was governed by the Jakob number. We used very low velocities ($v = 0.05 \text{ m s}^{-1}$) to reduce the drag force, and very low gravity fields (2% of earth gravity) to reduce the buoyancy force. These measures could be applied independently, and as already reported, there was no indication of 'sticking' affecting the overall bubble motion.

Anderson and Minns [17] hypothesised that, after a bubble was nucleated, microlayer evaporation would form a dry spot. The bubble would move away from the nucleation site, the dry spot would be re-wetted, and the bubble would slide over a continuous film of liquid. This hypothesis is supported by our observations.

7. CONCLUSIONS

Experiments were performed in which bubbles of vapour grew at a wall into an initially isothermal supersaturated liquid, with and without initial relative motion between liquid and wall, and also with gravity parallel to the wall varied from zero to earth gravity. The bubble movement is shown to be governed by its growth rate, by the motion in the liquid and by buoyancy, rather than by any 'sticking' of the bubble

due to surface tension acting at the wall. Certainly, when viewing the cine films there is no evidence of overall bubble motion being affected by sticking to the wall. Instead, the bubble appears to roll or slide along the wall, entraining a visible liquid wedge beneath it. Dry-out can occur over a small part of the bubble base, and that has often been expected to cause sticking, due to surface tension at its perimeter, but there does not appear to be any appreciable effect. These conclusions relating to the liquid wedge and the dried-out region are different from those by other workers. However, their experiments had temperature gradients near the wall, which can cause a 'mirage', preventing observation of these detailed phenomena at the wall.

The bubble does not move with the liquid or accelerate with gravity as freely as if the wall were absent. Approximate expressions can be set up to describe the motion of the bubble under the influence of growth, flow, and gravity, and combinations of these. The expression does not explicitly involve surface tension or viscosity, though the former must influence the shape, and there must be appreciable viscous stresses in the wedge between bubble and wall; that presumably reduces velocity and acceleration. The matter is complex, because the bubble presumably rolls along, i.e. fluid elements at the bubble surface do not all move at the mean velocity of the bubble. Drag coefficients for a sphere, which other workers have used in this context, are not considered appropriate, because they refer to drag in the presence of a fully developed wake. In our experiments, and in many applications, the downstream extremity of the bubble may move faster than the main stream for some time, and thereafter there is insufficient time for a wake to develop before departure.

Due to the rolling motion, departure from the wall is ill-defined. In studies by other workers, the mirage could also have led to an apparent time of departure from the wall which was in fact the time when the bubble broke completely through the thermal boundary layer. In the present work, times could be observed related to sliding or rolling departure, such as when the bubble base or the whole of the bubble had moved entirely beyond the original point of nucleation. For analysis of heat flow in boiling, it might be more useful to know the time and distance beyond which the bubble had little direct influence on heat flow. That is not a precise term, but an order of magnitude could be determined.

A more refined experiment would be needed to examine some aspects of the motion more closely, particularly when the bubble is much smaller than the velocity boundary layer, but the likely benefit to the understanding of boiling would not seem to warrant such examination.

The understanding of boiling is more likely to benefit from experiments combining the controlled velocity field of the present paper with a controlled temperature field, e.g. as in ref. [2], where it was found that departure occurred, unaided by gravity. Such experiments are planned.

Acknowledgement—One author (KM) acknowledges receipt of a scholarship from the Mitsui Engineering and Shipbuilding Co. Ltd., Japan. One author (CRS) acknowledges receipt of a grant from the S.E.R.C. and a Research Fellowship at Jesus College, Oxford, supported by the Leathersellers' Company. The work forms part of a study of the fundamentals of nucleate boiling, financed by the Engineering Sciences Division, A.E.R.E., Harwell.

REFERENCES

1. M. G. Cooper, A. M. Judd and R. A. Pike, Shape and departure of single bubbles growing at a wall, paper PB1, 6th Int. Heat Transfer Conf., Toronto, August (1978).
2. M. G. Cooper and T. T. Chandratilleke, Growth of diffusion-controlled vapour bubbles at a wall in a known temperature gradient, *Int. J. Heat Mass Transfer* **24**, 1475–1492 (1981).
3. R. Cole, Boiling nucleation, *Advances in Heat Transfer* Vol. 10. Academic Press, New York (1974).
4. M. G. Cooper and A. J. P. Lloyd, Miniature thin film thermometers with rapid response, *J. Scient. Instrum.* **42**, 791–793 (1965).
5. M. G. Cooper, A simple drop table for fractional gravity—design and instrumentation, *Int. J. Heat Mass Transfer* **26**, 1087–1088 (1983).
6. K. Mori, Behaviour of vapour bubbles growing at a wall with forced flow, M.Sc. Thesis, Oxford University, U.K. (1980).
7. G. K. Batchelor, *An Introduction to Fluid Dynamics*. Cambridge University Press (1970).
8. L. W. Florschuetz, C. L. Henry and A. Rashid Khan, Growth rates of free vapour bubbles in liquids at uniform superheats under normal and zero gravity conditions, *Int. J. Heat Mass Transfer* **12**, 1465–1489 (1969).
9. J. K. Walters and J. F. Davidson, The initial motion of a gas bubble in an inviscid liquid, Part 2, the three-dimensional bubble and the toroidal bubble, *J. Fluid Mech.* **17**, 321–336 (1963).
10. S. Levy, Forced convection subcooled boiling—prediction of vapour volumetric fraction, *Int. J. Heat Mass Transfer* **10**, 951–965 (1967).
11. N. Koumoustos, R. Moissis and A. Spyridonos, A study of bubble departure in forced-convection boiling, *J. Heat Transfer* **90**, 223–230 (1968).
12. F. C. Gunther, A photographic study of surface-boiling heat transfer to water with forced convection, *Trans. ASME* **83**, 115–123 (1951).
13. M. Akiyama and F. Tachibana, Motion of vapor bubbles in subcooled heated channel, *Bull. JSME* **17**, 241–247 (1974).
14. D. D. Williams and R. B. Mesler, The effect of surface orientation on delay time of bubbles from artificial sites during nucleate boiling, *A.I.Ch.E. JI* **13**, 1020–1024 (1967).
15. L. A. Skinner and S. G. Bankoff, Dynamics of vapour bubbles in general temperature fields, *Physics Fluids* **8**, 1417–1420 (1965).
16. G. J. Kirby, R. Staniforth and J. H. Kinneir, A visual study of forced convective boiling. Part I. Results for a vertical heater, AEEW-R281, AEE, Winfrith (1965).
17. G. H. Anderson and D. E. Minns, Nucleate boiling in a flowing liquid, in *Heat Transfer 1970*, 4th Int. H. T. Conf., B4.1 (1970).

COMPORTEMENT DE BULLES DE VAPEUR EN CROISSANCE SUR UNE PAROI AVEC UN ECOULEMENT FORCE

Résumé—On présente des expériences dans lesquelles des bulles individuelles croissent sur la paroi dans un liquide isotherme sursaturé se déplaçant par rapport à la paroi, avec un contrôle indépendant des champs de vitesse et de pesanteur. Des observations cinématographiques du mouvement de la bulle peuvent être expliquées simplement par des groupes adimensionnels concernant la croissance de la bulle, la vitesse du fluide et la pesanteur. Il n'y a pas d'indication que la tension interfaciale affecterait le mouvement global de la bulle à la paroi.

Des thermomètres sur la surface pariétale indiquent l'étendue de la région sèche sous la bulle et elle est trouvée plus faible que ne le suggèrent d'autres chercheurs. Les observations de ceux-ci peuvent avoir été affectées par un "mirage" causé par des variations d'indice de réfraction dans la couche limite thermique à la paroi.

VERHALTEN VON DAMPFBLASEN, WACHSTUM AN EINER WAND BEI ERZWUNGENER STRÖMUNG

Zusammenfassung—Die Experimente, über die berichtet wird, behandeln einzelne Dampfblasen, die an einer Wand entstehen und in eine anfangs isotherme überhitzte Flüssigkeit, die sich gegenüber der Wand bewegt, hineinwachsen. Dabei sind Geschwindigkeits- und Schwerfeld unabhängig voneinander einstellbar. Filmaufnahmen von der Blasenbewegung könnten einfach mittels dimensionsloser Kennzahlen beschrieben werden. Diese enthalten Blasenwachstum, Flüssigkeitgeschwindigkeit und Schwerkraft. Es gab keine Anzeichen dafür, daß die Oberflächenspannung die resultierende Blasenbewegung beeinflusst, indem Blasen an der Wand 'festkleben'. Thermometer an der Wandoberfläche zeigten die Ausdehnung des Bereichs der trockenen Wand unter einer Blase; wobei sich herausstellte, daß dieser Bereich kleiner ist als in anderen Arbeiten angenommen. Die Beobachtungen in früheren Arbeiten könnten auf einer Täuschung beruhen, die durch die Änderung des Brechungsindex in der thermischen Grenzschicht an der Wand verursacht wurde.

ПОВЕДЕНИЕ РАСТУЩИХ НА СТЕНКЕ ПУЗЫРЬКОВ ПАРА ПРИ ВЫНУЖДЕННОМ ТЕЧЕНИИ

Аннотация—Описаны эксперименты, в которых отдельные пузырьки растут на стенке в первоначально изотермической перенасыщенной жидкости, движущейся относительно стенки, при автономном управлении полями скорости и силы тяжести. Данные кино съемки движения пузырьков можно просто описывать безразмерными критериями, включающими рост пузырьков, скорость жидкости и силу тяжести. Влияния поверхностного натяжения на суммарное движение пузырьков, проявляющееся в 'прилипании' их к стенке, не обнаружено. Термометрами, установленными на поверхности стенки, определялся размер сухой области под пузырьками, величина которого оказалась ниже значений, сообщаемых другими авторами. Эти данные могли оказаться выше из-за влияния 'миража', вызываемого изменением коэффициента преломления в тепловом пограничном слое на стенке.